

High flame retardancy of amorphous sodium silicate on poly(ethylene-*co*-vinyl acetate) (EVA)

Isao Tsuyumoto¹ 

Received: 11 July 2017 / Revised: 23 January 2018 / Accepted: 12 March 2018 /
Published online: 15 March 2018
© Springer-Verlag GmbH Germany, part of Springer Nature 2018

Abstract Amorphous sodium silicate (ASL) is found to show high flame retardancy on poly(ethylene-*co*-vinyl acetate) (EVA), in contrast to crystalline sodium disilicate, $\text{Na}_2\text{Si}_2\text{O}_5$, with similar composition. The EVA polymer (ethylene content: 67 wt%) loaded with 33 wt% or more of ASL shows self-extinguishing properties and meets the UL94V-0 rating, while the EVA polymer loaded with 33 wt% of the crystalline $\text{Na}_2\text{Si}_2\text{O}_5$ does not even meet the UL94 HB rating. The flame retardant effect of ASL is much higher than the conventional halogen-free additives such as magnesium hydroxide. The TG measurements of the flame retardant EVA samples and the scanning electron microscope observations of the combustion residues suggest that the remarkable flame retardancy is due to the film-forming properties of ASL.

Keywords Flame retardancy · EVA · Silicate

Introduction

Flame retardant treatments are essential for polymer materials to prevent fire disasters, because their heat release after ignition increases rapidly. A wide variety of flame retardants have been developed and used in the polymer materials of household appliances, buildings, automobiles, trains, and cables. Halogen- or phosphorus-based flame retardants, however, cause environmental concerns, because they are toxic in most cases and toxic products may be released in fire,

✉ Isao Tsuyumoto
tsuyum@neptune.kanazawa-it.ac.jp

¹ Department of Applied Chemistry, College of Bioscience and Chemistry, Kanazawa Institute of Technology, 7-1 Ohgigaoka, Nonoichi, Ishikawa 921-8501, Japan

disposal, and ordinary use [1]. Magnesium hydroxide and aluminium hydroxide have been widely used as halogen- and phosphorus-free additives in polyolefin polymers, e.g., poly(ethylene-*co*-vinyl acetate) (EVA) for manufacturing cables, but such inorganic hydroxides need to be added in large quantities by 50 wt% or more to achieve the practical level of flame retardancy. Boehmite, $\text{AlO}(\text{OH})$ and hydrotalcite, $\text{Mg}_4\text{Al}_2(\text{CO}_3)(\text{OH})_{12}\cdot 3\text{H}_2\text{O}$ have been reported as alternative halogen- and phosphorus-free flame retardant additives for EVA [2], and zinc borates have been reported to be synergistic agents in flame-retardant aluminium hydroxide- or magnesium hydroxide-filled EVA [3]. However, such additives are needed in large quantities as ever to achieve the practical level of flame retardancy. New halogen- and phosphorus-free flame retardants are still highly desirable, while other new halogen- and phosphorus-free flame retardants have been also reported so far for various polymer materials [4], e.g., expandable graphite [5], organically modified montmorillonite [6], triazinic polyol [7].

Our research group has reported the remarkable flame-retardant effects of amorphous sodium borate on polymer materials such as nonwovens of ethylene–vinyl alcohol copolymer (EVOH) and poly(ethylene terephthalate) (PET) [8], rigid polyurethane foam (RPU) [9, 10], laminated wood [11]. Amorphous sodium borate was introduced inside the materials by impregnation of a concentrated sodium polyborate solution. The dry residue of the solution was an amorphous phase of sodium borate, and the amorphous phase was found to show higher flame-retardant effects than crystalline phases such as sodium tetraborate decahydrate (borax), boric acid. It is generally known that borate shows similar behavior as silicate, and silicate is far more abundant than borate on the earth. The production cost and environmental load of the flame retardants will be reduced by developing silicate-based flame retardants of the similar performance.

Sodium silicate solution (water glass) has been widely used as a flame retardant and an adhesive of cellulose-based materials such as paper, cardboard, plywood, and cotton fabrics [12–15]. Silica and silicone resin have also been used for flame-retardant additives of polymer materials [16, 17]. On the other hand, sodium silicate powder has not been applied to the flame-retardant additives of the polymer materials, and there have been no reports on the flame retardant effects of sodium silicate powder when melt-mixed with the polymer materials. Considering the fact that some kinds of polymer materials show flame retardancy by coating with sodium silicate-based solution, sodium silicate powder is expected to give flame retardancy to the polymer materials by melt-mixing. Sodium silicate powder is advantageous over the other additives, because it contains no hazardous elements and is made from abundant natural resources.

This study focused on the potential application of sodium silicate powder to the flame retardants of EVA. The aim is to investigate the relationship between the flame retardancy and the character of sodium silicate.

Experimental

Materials

Amorphous sodium silicate (ASL) was prepared by drying a sodium silicate solution (17.7 wt% Na₂O, 36.9 wt% SiO₂, 45.4 wt% H₂O, Na/Si molar ratio 0.93, density 1.70 g/cm³, Fuji Kagaku, Osaka, Japan) at 200 °C for 24 h. Crystalline sodium disilicate, Na₂Si₂O₅, was prepared by drying the same solution at 200 °C for 14 days or more. Each sodium silicate sample after drying was crushed into fine powder using mortar and pestle.

EVA used in the present study was a commercially available extrusion-grade (EV170, Du Pont-Mitsui Polychemicals, Tokyo, Japan) with ethylene content of 67 wt%, melting point of 62 °C, and melt flow rate (MFR) of 1 g/10 min (at 190 °C and a load of 2.16 kg). The EVA pellet was melt-mixed with the sodium silicate powder using a counter-rotating twin-screw mixer (Musashino Kikai, Tokyo, Japan) at 80 °C and 60 rpm for 15 min. The formulations of the EVA–ASL mixtures were in the range of 91 wt% EVA–9 wt% ASL to 50 wt% EVA–50 wt% ASL. For comparison, the mixtures of 67 wt% EVA–33 wt% crystalline Na₂Si₂O₅ and 67 wt% EVA–33 wt% Mg(OH)₂ were also prepared. Sample pieces in size of 125 mm × 13 mm × 3 mm were fabricated by hot-press molding at 80 °C and 10 MPa for 5 min.

Measurement

The crystal structures of the sodium silicates were identified by the powder X-ray diffraction (XRD) measurements (XD-D1, Shimadzu, Kyoto, Japan) using graphite monochromatized Cu K α radiation ($\lambda = 0.154059$ nm) at 30 kV and 30 mA. The X-ray profiles were collected between 2° and 120° with a step interval of 0.02° and a count time of 1 s/step. The differential thermal analysis and thermogravimetry (DTA/TG, DTG-60, Shimadzu, Kyoto, Japan) was performed for the sodium silicates and the flame retardant EVA in air at a heating rate of 20 °C/min. The sodium silicates were measured after drying at 200 °C for specified time and crushing into fine powder using mortar and pestle. As for the flame retardant EVA, 4–6 mg of the sample was cut from the whole specimen and used for the measurement. Flame retardant effect was evaluated according to the American National Standard UL 94 (ASTM D635-14, D3801-10) using rectangular samples of EVA in size of 125 mm × 13 mm × 3 mm [18]. The surface morphology of the samples after the combustion tests was investigated using a scanning electron microscope (SEM, JSM-5610, JEOL, Tokyo, Japan) with an accelerating voltage of 10 kV.

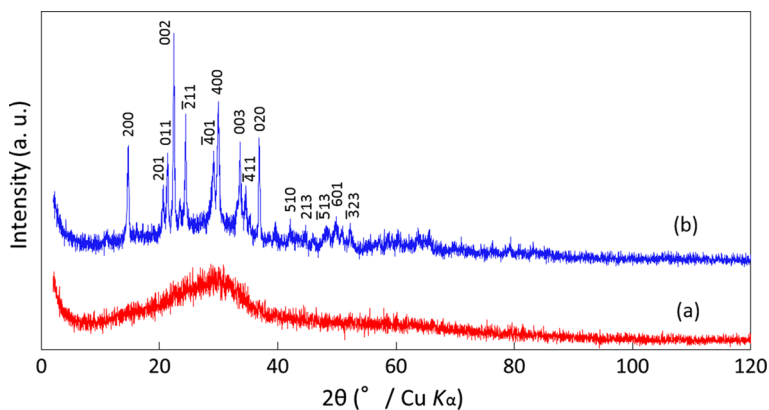


Fig. 1 XRD patterns of the sodium silicates obtained by drying the sodium silicate solutions at 200 °C for **a** 24 h and **b** 14 days

Results and discussion

Figure 1 shows the XRD patterns of sodium silicates obtained by drying the sodium silicate solution at 200 °C for 24 h and 14 days. Only one broad peak was observed in Fig. 1a, and this indicates that drying the sodium silicate solution for 24 h yielded an amorphous sodium silicate. In Fig. 1b, the sharp peaks emerged by extending the drying time to 14 days, and the peaks were assigned as β - $\text{Na}_2\text{Si}_2\text{O}_5$ (sodium disilicate, natrosilite) reported in the literature (PDF4 00-029-1261). The crystalline phase of β - $\text{Na}_2\text{Si}_2\text{O}_5$ was found to form by drying the sodium silicate solution for 14 days. Since the Na/Si molar ratio of the sodium silicate solution is 0.93, the crystalline phase of β - $\text{Na}_2\text{Si}_2\text{O}_5$ should form with some fraction of the other phase (Na/Si < 0.93). Because all the sharp peaks in Fig. 1b are assigned as β - $\text{Na}_2\text{Si}_2\text{O}_5$, some fraction of amorphous phase is considered to remain with crystalline β - $\text{Na}_2\text{Si}_2\text{O}_5$. These two samples were fine white powders showing no difference in their appearance and texture. The TG curve of the amorphous sodium silicate showed a weight decrease by 5.8% from 200 to 860 °C and a melting point at 855 °C, while that of the crystalline $\text{Na}_2\text{Si}_2\text{O}_5$ showed the same melting point at 855 °C and a smaller weight change, 1.9%, as shown in Fig. 2. This indicated that the amorphous sodium silicate contained 5.8 wt% of hydrated water and the crystalline $\text{Na}_2\text{Si}_2\text{O}_5$ contained less hydrated water. The DTA/TG curves for the two samples did not show much difference except for the amount of water release. The type of the product can be controlled by changing the drying time, and this is in agreement with the reported phase diagram of Na_2O – SiO_2 – H_2O [19]. Additionally, to our knowledge, all commercially available sodium silicate powders were crystalline phases.

Table 1 summarizes the combustion properties of the EVA samples melt-mixed sodium silicates in the UL 94 test. A remarkable difference in flame retardancy on EVA was observed between the amorphous sodium silicate and the crystalline one. The sample of 67 wt% EVA–33 wt% crystalline $\text{Na}_2\text{Si}_2\text{O}_5$ and the virgin EVA

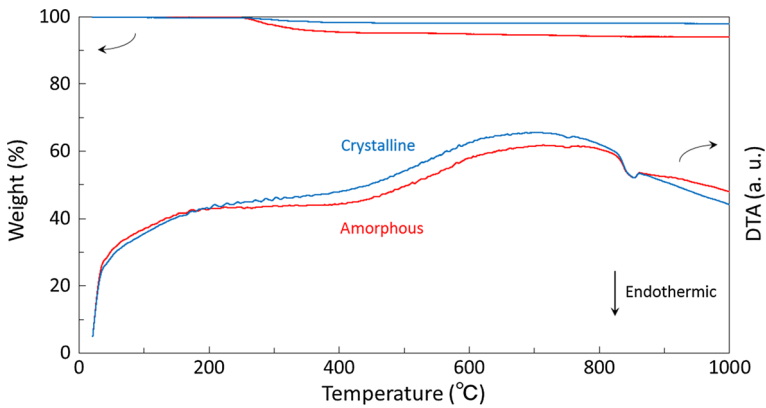


Fig. 2 DTA/TG curves for the sample powders of ASL and crystalline $\text{Na}_2\text{Si}_2\text{O}_5$ in air

Table 1 Combustion properties of the EVA samples melt-mixed with the sodium silicates in the UL94 test

Additive	Loading (wt%)	UL94	Horizontal burning rate (mm/min)	Dripping
None	0	–	102	Yes
ASL	9	–	75	No
ASL	17	–	65	No
ASL	23	–	63	No
ASL	29	HB	35	No
ASL	33	V-0	–	No
ASL	38	V-0	–	No
ASL	41	V-0	–	No
ASL	44	V-0	–	No
ASL	47	V-0	–	No
ASL	50	V-0	–	No
$\text{Na}_2\text{Si}_2\text{O}_5$	33	–	79	Yes
$\text{Mg}(\text{OH})_2$	33	–	225	Yes

showed dripping and burning rates greater than 40 mm/min in the horizontal burning (UL 94 HB) test, which did not satisfy the UL 94 HB requirements. In contrast, dripping was not observed for the EVA samples containing 9 wt% or more of ASL, and notably the EVA samples containing 33% or more of ASL achieved the UL 94V-0 standard. Self-extinguishing properties were observed for the samples containing 33% or more of ASL in both the UL 94 HB and V-0 tests, while the sample containing 29% of ASL did not show the self-extinguishing properties and met the UL 94 HB standard. The EVA samples containing 33% or more of ASL burned with a small flame with length of 1–2 cm before the self-extinguishing, while the flame of that with the crystalline $\text{Na}_2\text{Si}_2\text{O}_5$ was over 10 cm in length.

Additionally, 67 wt% EVA–33 wt% $\text{Mg}(\text{OH})_2$ sample showed dripping and did not meet the UL 94 HB nor V-0 standards. It can be said that ASL has much greater flame retardancy on EVA compared with the conventional $\text{Mg}(\text{OH})_2$.

Figure 3 shows the appearance of the combustion residues after the UL 94 HB tests. Black char remained with white powder on it, and the white powder covering the black char spread with increasing the content of ASL. It is considered that the white powder covering the black char brought about the self-extinguishing phenomena of the samples containing ASL by 33% or more. The content of hydrated water in ASL was as small as 5.8%, and this is much smaller than that of constitution water in $\text{Mg}(\text{OH})_2$, 30.9%, which is calculated from the theoretical weight decrease when $\text{Mg}(\text{OH})_2$ decomposes into MgO and H_2O . Thus, the great flame retardancy is neither due to the cooling effect nor gas dilution effect of hydrated water because such effects of hydrated water in ASL should be much smaller than that of $\text{Mg}(\text{OH})_2$. As for the EVA–ASL mixtures, gasification burning is considered to be suppressed by other mechanism. Figure 4 shows the SEM images of the carbonized regions of the sample residues. The white powder on the surface of the black char of the EVA–ASL samples was the flakes and foam of ASL as shown in Fig. 4a, and these protected the char from oxygen and heat. Such flakes and foam were observed a little for the crystalline $\text{Na}_2\text{Si}_2\text{O}_5$, and the foam was isolated and did not link together, as shown in Fig. 4b. It is important to establish the network of foamed structure by linking together throughout the overall specimen like percolation for the flame retardancy, and this depends on the fraction of the ASL. A little foam observed for the crystalline $\text{Na}_2\text{Si}_2\text{O}_5$ is considered to be derived from the remaining fraction of the amorphous phase. The remarkable difference in the flame retardancy between the EVA samples containing 29 and 33% of ASL in Table 1 and Fig. 3 presumably depend on whether or not the network of the foamed structure is formed throughout the overall specimen. The observed self-extinguishing properties are due to this shielding effect of the network of the flakes and foam,

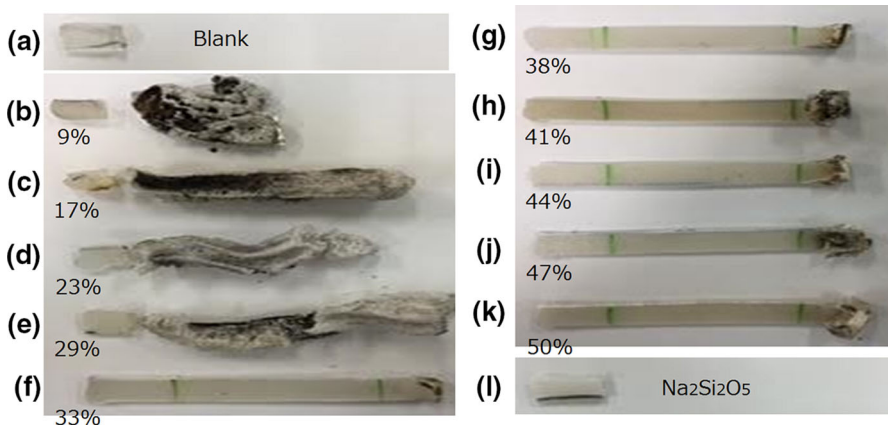


Fig. 3 Appearance of the combustion residues after the UL 94 HB test. The flame was applied to the right ends of the samples. Their ASL contents (wt%) are shown together

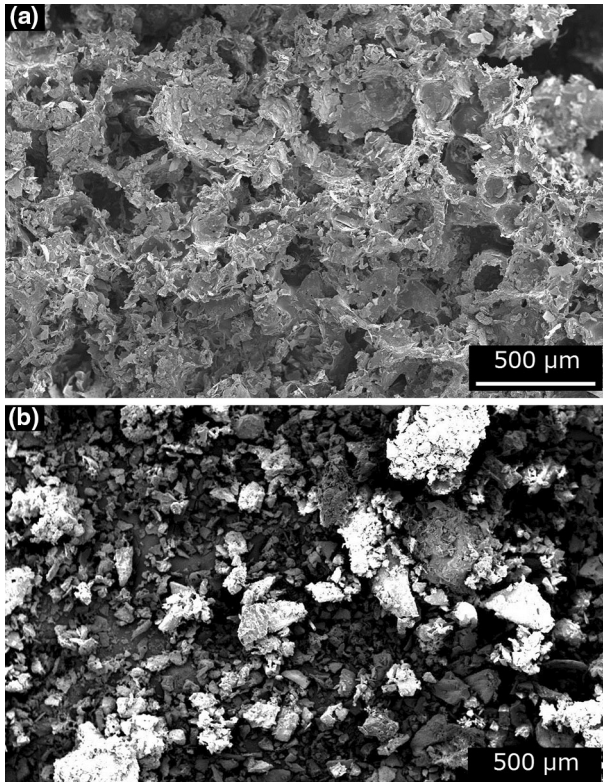


Fig. 4 SEM images of the carbonized regions of the sample residues. Each EVA sample was melt-mixed with 33 wt% of **a** ASL and **b** crystalline $\text{Na}_2\text{Si}_2\text{O}_5$

and this is the first observation of an intumescent-like flame retardant effect of the amorphous sodium silicates.

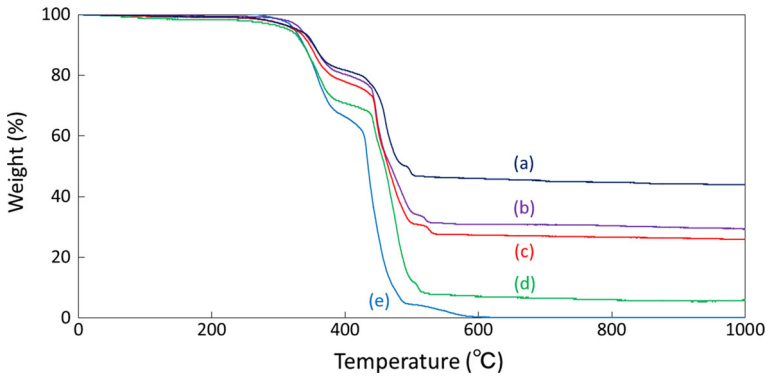


Fig. 5 TG curves of the formulations EVA–ASL and EVA–crystalline $\text{Na}_2\text{Si}_2\text{O}_5$ in comparison with the virgin EVA. **a** 50 wt% ASL, **b** 33 wt% crystalline $\text{Na}_2\text{Si}_2\text{O}_5$, **c** 33 wt% ASL, **d** 9 wt% ASL, and **e** virgin EVA

Figure 5 shows the TG curves of the EVA samples containing ASL (9, 33, and 50 wt%) and crystalline $\text{Na}_2\text{Si}_2\text{O}_5$ (33 wt%) along with the virgin EVA. The thermal degradation of EVA has been reported to proceed in three stages. The first stage (250–350 °C) can be assigned to the evolution of acetic acid due to the decomposition of the vinyl acetate groups [3, 20]. The second stage (425–500 °C) corresponds to the degradation of the polyethylene chains [3, 20, 21]. The third stage (550–600 °C) may be assigned to the oxidation of carbonaceous residue [3]. The thermal degradation behaviors of our samples corresponded with those reported in the literature. The first-stage degradation of the flame-retardant samples started at lower temperature than the virgin sample and ceased at almost the same temperature as the virgin sample. In this stage, the evolution of combustible degradation products such as acetic acid does not enhance the combustibility because the temperature is below their ignition points. The gas emission below the ignition points at early stage may be favorable to the flame retardancy. The second-stage degradation of the flame retardant samples occurred at a little higher temperature region than the virgin sample, and the temperature region was gradually increased with increasing flame-retardant additives. In this stage, the flame retardant additives are considered to affect the mechanism of gasification and carbonization, i.e., suppress gasification burning and enhance carbonization. In the third stage, weight decrease due to the oxidation of carbonaceous residue ceased faster compared with the virgin sample. This suggests the formation of incombustible char from the flame-retardant samples instead of combustible carbonaceous substance. It is noteworthy that the EVA samples containing 33 wt% ASL and 33 wt% crystalline $\text{Na}_2\text{Si}_2\text{O}_5$ showed almost the same TG curves, though their flame retardancies were remarkably different. The slight deviation between the two curves is due to the hydrated water content of ASL. The correspondence of the two TG curves suggests that the remarkable flame retardancy is due to not only the changes in the thermal degradation behaviors but also changes in the mechanical properties of EVA matrix brought by the amorphous network of ASL such as melt viscosity increase and the suppression of dripping.

It is considered that the remarkable flame-retardant effect as well as the dripping suppression is due to film-forming properties of the amorphous phase. The amorphous sodium silicate, a highly viscous glass, constructs a network in the polymer matrix and transforms into glass film when heated. The glass film, swollen by decomposition gas, subsequently changes into the glass foam. The stiffness of the glass network suppresses the dripping, and the glass film (flakes) and foam shield the polymer matrix from oxygen and heat. Carbonized layers made from polymer matrix also protect inside from oxygen and heat. This flame retardant mechanism is similar to those of the intumescent flame retardants, though the expansibility is apparently lower. Generally, such effects are not expected for pulverized crystalline phases, since they only keep existing as powders in polymer matrix. Our results give a new design guideline of flame retardants that amorphous phases are advantageous over the crystalline phases with similar compositions.

Conclusions

A remarkable flame retardant effect of ASL on EVA was found. Self-extinguishing was observed for EVA samples melt-mixed with ASL by 33 wt% or more, and dripping was thoroughly suppressed for the EVA samples melt-mixed by 9 wt% or more. The amorphous sodium silicate is considered to transform into glass film and foam on sample surfaces when heated, and these as well as carbonized layers protect polymer matrix inside from heat and oxygen. Dripping is also suppressed by the stiffness of glass network in the polymer matrix. Our findings are solely due to using amorphous sodium silicate instead of crystalline ones, and this suggests that new properties can be expected even for well-known conventional flame-retardant additives by controlling their crystallinity and structures.

Acknowledgements The author is grateful to Messrs. Ryo Kuwata, Kohei Matsumoto, and Fumiki Goto for their assistance in the experiments in this work. This work was supported by a Grant-in-Aid for Scientific Research (C), KAKENHI, no. 16K05946, from the Japan Society for the Promotion of Science (JSPS).

References

1. Purser D (2000) The performance of fire retardants in relation to toxicity, toxic hazard, and risk in fires. In: Grand AF, Wilkie CA (eds) Fire retardancy of polymeric materials, vol 12. Marcel Dekker, New York, p 449
2. Camino G, Maffezzoli A, Braglia M, De Lazzaro M, Zammarano M (2001) Effect of hydroxides and hydroxycarbonate structure on fire retardant effectiveness and mechanical properties in ethylene–vinyl acetate copolymer. *Polym Degrad Stab* 74(3):457–464
3. Bourbigot S, Le Bras M, Leeuwendal R, Shen KK, Schubert D (1999) Recent advances in the use of zinc borates in flame retardancy of EVA. *Polym Degrad Stab* 64(3):419–425
4. Lu SY, Hamerton I (2002) Recent developments in the chemistry of halogen-free flame retardant polymers. *Prog Polym Sci* 27:1661–1712
5. Thirumal M, Khashtgir D, Singha NK, Manjunath BS, Naik YP (2008) Effect of expandable graphite on the properties of intumescent flame-retardant polyurethane foam. *J Appl Polym Sci* 110:2586–2594
6. Song R, Wang Z, Meng X, Zhang B, Tang T (2007) Influence of catalysis and dispersion of organically modified montmorillonite on flame retardancy of polypropylene nanocomposites. *J Appl Polym Sci* 106:3488–3494
7. Ionescu M, Mihalache L, Zugravu V, Mihai S (1994) Inherently flame retardant rigid polyurethane foams based on new triazinic polyether polyols. *Cell Polym* 13:57–68
8. Tsuyumoto I, Miura Y, Hori Y (2010) Fire resistant nonwovens of EVOH and PET treated with amorphous sodium polyborate. *J Mater Sci* 45:2504–2509
9. Tsuyumoto I, Onoda Y, Hashizume F, Kinpara E (2011) Flame retardant rigid polyurethane foams prepared with amorphous sodium polyborate. *J Appl Polym Sci* 122:1707–1711
10. Tsuyumoto I, Miura Y, Nirei M, Ikurumi S, Kumagai T (2011) Highly flame retardant coating consisting of starch and amorphous sodium polyborate. *J Mater Sci* 46:5371–5377
11. Tsuyumoto I, Oshio T (2009) Development of fire resistant laminated wood using concentrated sodium polyborate aqueous solution. *J Wood Chem Technol* 29:277–285
12. Nassar MM, Fadali OA, Khattab MA, Ashour EA (1999) Thermal studies on paper treated with flame-retardant. *Fire Mater* 23:125–129
13. Pereyra AM, Giudice CA (2009) Flame-retardant impregnants for woods based on alkaline silicates. *Fire Saf J* 44:497–503
14. Medina LA, Schledjewski R (2009) Water glass as hydrophobic and flame retardant additive for natural fibre reinforced composites. *J Nanostruct Polym Nanocompos* 5:107–114

15. Kumar SP, Takamori S, Araki H, Kuroda S (2015) Flame retardancy of clay-sodium silicate composite coatings on wood for construction purposes. *RSC Adv* 5:34109–34116
16. Kashiwagi T, Gilman JW, Butler KM, Harris RH, Shields JR, Asano A (2000) Flame retardant mechanism of silica gel/silica. *Fire Mater* 24:277–289
17. Berta M, Lindsay C, Pans G, Camino G (2006) Effect of chemical structure on combustion and thermal behaviour of polyurethane elastomer layered silicate nanocomposites. *Polym Degrad Stab* 91:1179–1191
18. UL94 (2009) Test for flammability of plastic materials for parts in devices and appliances. Underwriters Laboratories Inc, USA
19. Weldes HH, Lange KR (1969) Properties of soluble silicates. *Ind Eng Chem* 61:29–44
20. Costello CA, Schultz DN (1986) Kirk-Othmer encyclopedia of chemical technology, 4th edn. Wiley/Interscience, New York, pp 349–381
21. Gardner DL, McNeill IC (1969) Investigations of thermal elimination reactions of polymers by thermal volatilization analysis and ultraviolet spectroscopy. *J Therm Anal* 1(4):389–402